International Journal of Electrical, Electronic and Communication Sciences
ISSN: 2517-9438
Vol:11, No:6, 2017

Thermal and Flammability Properties of Paraffin/Nanoclay Composite Phase Change Materials Incorporated in Building Materials for Thermal Energy Storage

Awni H. Alkhazaleh, Baljinder K. Kandola

***Abstract*—**In this study, a form-stable composite Paraffin/Nanoclay (PA-NC) has been prepared by absorbing PA into porous particles of NC to be used for low-temperature latent heat thermal energy storage. The leakage test shows that the maximum mass fraction of PA that can be incorporated in NC without leakage is 60 wt.%. Differential scanning calorimetry (DSC) has been used to measure the thermal properties of the PA and PA-NC both before and after incorporation in plasterboard (PL). The mechanical performance of the samples has been evaluated in flexural mode. The thermal energy storage performance has been studied using a small test chamber (100 mm × 100 mm × 100 mm) made from 10 mm thick PL and measuring the temperatures using thermocouples. The flammability of the PL+PL-NC has been discussed using a cone calorimeter. The results indicate that the form composite PA has good potential for use as thermal energy storage materials in building applications.

***Keywords*—**Flammability, paraffin, plasterboard, thermal energy storage.

I. Introduction

THERMAL energy storage using phase change materials (PCMs) has received great attention recently in attempts to improve building energy efficiency. Thermal energy storage can be achieved by three methods [1], [2], namely sensible heat storage, latent heat storage, and chemical energy storage. Latent heat energy storage is widely used in engineering applications to conserve energy, reduce the dependence on oil, and shift the energy from peak load period to off-peak load period. The PCMs whose low melting temperature is close to human comfort temperature ~24 °C have been considered to be used in building applications [3], [4]. PA is one of the most significant PCMs [5] due to a huge latent heat, varied melting temperature depending on structure, relatively low cost, non-toxicity, and chemical stability. Heat can be absorbed when the material changes its phase from solid to liquid during the daytime (high temperature) and released at night (low temperature) when the material changes its phase from liquid to solid. There are three techniques of integrating PCM into building materials, immersion, direct incorporation, and form-stable composite PCM [6]. In immersion technique, the leakage of the liquid PA to the surface of building materials is unavoidable particularly when the PA is heated above its melting temperature.

To overcome the leakage problem of PA in immersion technique [7] and improve the consistency of organic PA with plaster, the novel route of incorporating PA into plaster is carried out using NC. PA is successfully mixed and held in the porous NC. On the other hand, when the PA integrates into building materials [8] such as concrete, gypsum board, and plaster, the most significant concern is its flammability. In the event of a fire, the PA containing building material burns and a significant amount of toxic gases, smoke, and flame can be generated [9], [10]. The fire can transfer simply from the point of origin to adjacent spaces [11]-[14] and can cause great number of fatalities, injures, and economic loss.

Awni H. Alkhazaleh and Baljinder K. Kandola are with School of Engineering, Institute for Materials Research and Innovation, University of Bolton, Manchester, UK (e-mail: awnialkhazaleh@gmail.com).

II. Materials and Experimental

A. Materials

1. Gypsum Powder

Gypsum powder used in this project was sourced from British Gypsum, British Gypsum Thistle Multi Finish was used as received. The general composition provided by manufacture is that it mainly contains calcium sulfate hemihydrate. Other constituents such as clay, limestone (calcium carbonate) and minor amounts of quartz and hydrated lime are also present.

2. Paraffin

N-octadecane (PA), 99% with melting temperature range of 26-29 °C was sourced from Alfa Aesar.

3. Nanoclay

Commercial NC, 20A, with particle size of 0.2 mm was supplied by BYK additives and instruments UK.

B. Preparation of the Form-Stable PA-NC Composite

In this work, the novel composite PA-NC was prepared by adsorbing PA into the NC. PA was melted at temperature of 40 °C for 30 min in an oven and then different mass fractions of PA (20, 30, 40, 50, 60, 70, 80 wt %) were immediately mixed with NC at room temperature. The optimum mass fraction of PA without leakage was found to be 60 wt.%, the image of sample is shown in Fig. 1. The leakage test was

applied by heating the blend at least 10 °C above the melting temperature of PA in order to observe visually if there was any leakage. In order to obtain fine particles of blend, blend was placed into freezer for 20 min, after cooling; the blend was ground by mill.

Fig. 1 Digital image of form-stable composite of 60% PA-40% NC

10 wt.% of PA in the blend of 16.7 wt.% of PA-NC was firstly mixed with gypsum powder before making slurry and then the water is added. A handheld electric mixer was used until a uniform blend was achieved. Then, the prepared slurry was poured in a wooden mould of dimensions 100 mm x 100 mm x 10 mm and the mould was placed at room temperature for 14 days to dry, the image of the prepared sample is shown in Fig. 2.

Fig. 2 Digital image of PL containing form-stable PA-NC

C. DSC

The phase change properties of composite were characterized using DSC. The DSC thermal analysis has been accomplished in the temperature range of 0-40 °C with heating and cooling rate of 3 °C/min under constant stream of nitrogen at atmospheric pressure.

D. Mechanical Performance of Flexural Properties

The flexural properties of PL samples with/without PA-NC composite were tested in three point bending mode. Three replicate specimens of the size of 130 mm x 130 mm x 10 mm were tested for each sample. Loading was applied by adding weights gradually until failure (when the specimen could not carry any more load and broke). The flexural strength σ_f is expressed in (1):

$$\sigma_f = \frac{MY}{I} \quad (1)$$

where σ_f is the stress in the outer surface at the middle point, M is the moment applied at the middle of the specimen, Y is the distance from the outer surface to the centre of specimen, and I is the polar moment of inertia of rectangular cross sectional area.

E. Cone Calorimeter Test

The cone calorimeter test was performed according to the procedures representing in the ISO 5660-1 standard using a Fire Testing Technology cone calorimeter with slight modifications on the methodology and sample holder [9]. The vertical orientation of cone calorimeter has been used and the tested samples were vertically mounted. The ignition source used in this experiment was spark. Three specimens of each sample with dimensions of 75 mm x 75 mm x 10 mm have been tested instead of using the standard dimensions of 100 mm x 100 mm x 10 mm due to the limitation in the quantity of materials available. The fire behavior of control PL and PL+PA-NC have been performed using heat flux of 70 kW/m^2.

F. Thermal Energy Storage Performance

Small test room of PL with dimension of 100 mm x 100 mm x 100 mm and thickness 10 mm was set up using six pieces of PL. The top board and left side of cubic room were achieved by form-stable composite PA techniques. To compare the temperature difference between control PL and PL+PA-NC, a small environmental chamber was used. Two thermocouples were placed at different locations: bottom of top board (T1) and middle of cube (T2) as shown in Fig. 3. These thermocouples were linked to a data acquisition to record the temperatures of the test room during the test. The thermal energy storage performance has been evaluated in heating and cooling modes. The chamber was switched on for 1 h before testing in order to set up the temperature inside chamber to be at room temperature 20 °C. In heating mode, the samples have been heated from 20 °C (room temperature) to 50 °C for 55 min with heating rate of 0.54 °C/min and the temperature was kept at 50 °C for 25 min. In cooling mode, the samples were cooled from 50 °C to 6 °C for 95 min with cooling rate of 0.46 °C/min and the temperature was kept at 6 °C for 25 min. The temperature and time were recorded for 200 min.

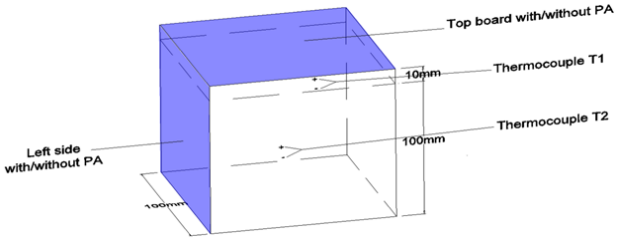

Fig. 3 Small test room to evaluate the thermal energy performance

III. Results and Discussion

A. DSC

The thermal properties of PA, PA-NC and PL+PA-NC measured by DSC are shown in Fig. 4. There is an endothermic peak during the heating process which represents solid-liquid phase change. During cooling process, there is an exothermic peak which represents the liquid-solid phase

change. The melting and freezing temperatures of PA were measured to be 27.69 °C and 27.07 °C, respectively as depicted in Fig. 4 (a), which were in the range of thermal comfort temperature.

The latent heats of melting and of freezing temperatures were found to be 243 J/g and 250 J/g, respectively, which suggest that the PA has a large latent heat to be applied for thermal energy storage applications. As can be clearly seen from Fig. 4 (b), the melting and freezing temperatures of PA-NC were 27.47 °C and 27.06 °C, respectively. Both of melting and freezing temperatures of PA in the composite are almost the same as that observed in PA and are in the range of human comfort temperature. Moreover, the latent heats of melting and of freezing temperatures of PA in the composite of PA-NC were determined to be 143.5 J/g and 140.7 J/g, respectively. Its calculated latent heats based on the mass fraction of PA in the PA-NC are almost similar to that of measured latent heat values by DSC, they are 239.2 J/g and 234.5 J/g, respectively. These results indicate that the measured latent heat of PA in the composite by DSC is in agreement with the optimum mass fraction of PA mixed with NC.

In terms of the thermal properties of PA in the composite of PL+PA-NC (see Fig. 4 (c)), the melting and freezing temperatures measured by DSC are 27.37 °C and 27.17 °C, respectively, which are almost similar to that of pure PA and PA-NC. Furthermore, the latent heats of melting and of freezing temperatures of PA in the composite have significantly reduced to 12.93 J/g and 12.84 J/g, respectively. However, its calculated latent heats based on the mass fraction of PA are 129.3 J/g and 128.4 J/g, respectively. The mass fraction of PA added in PL+PA-NC is 10 wt.% and the latent heat of fusion in the composites with/without plaster is provided only by PA.

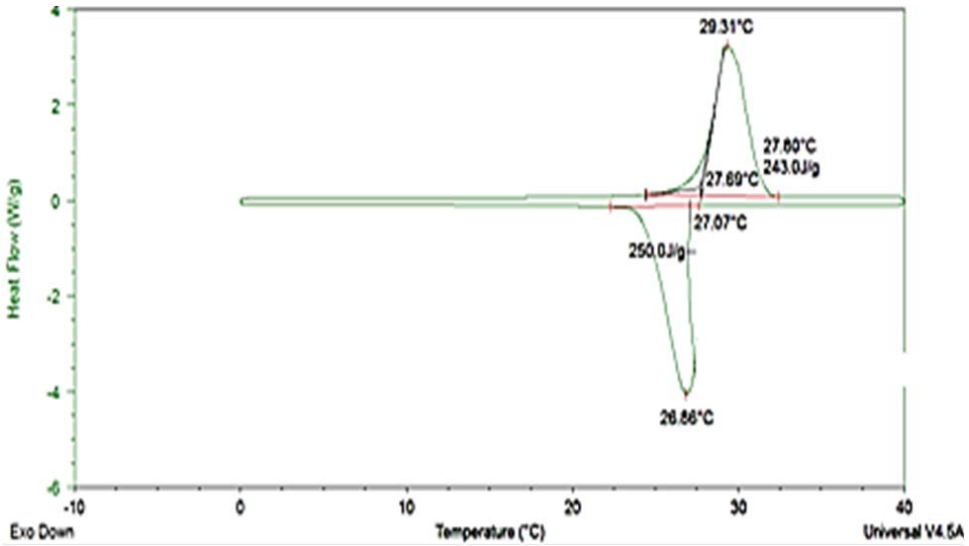

(a)

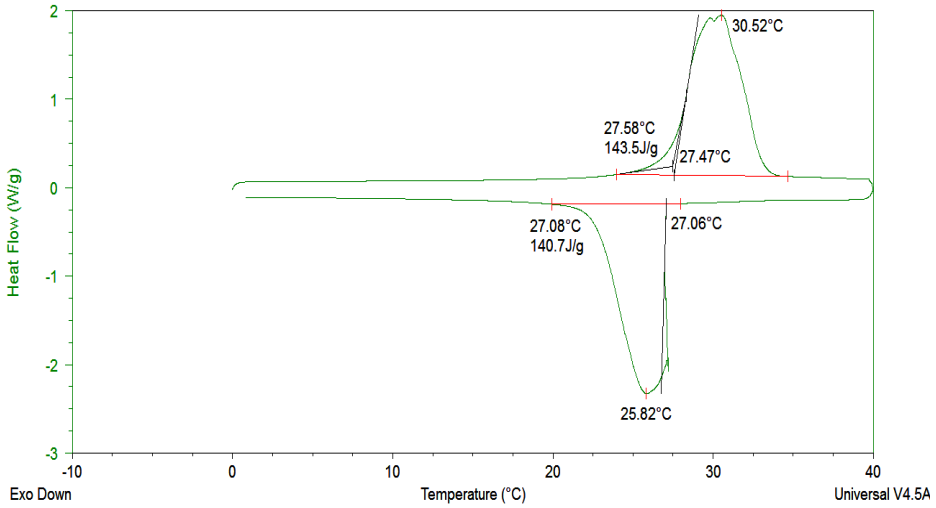

(b)

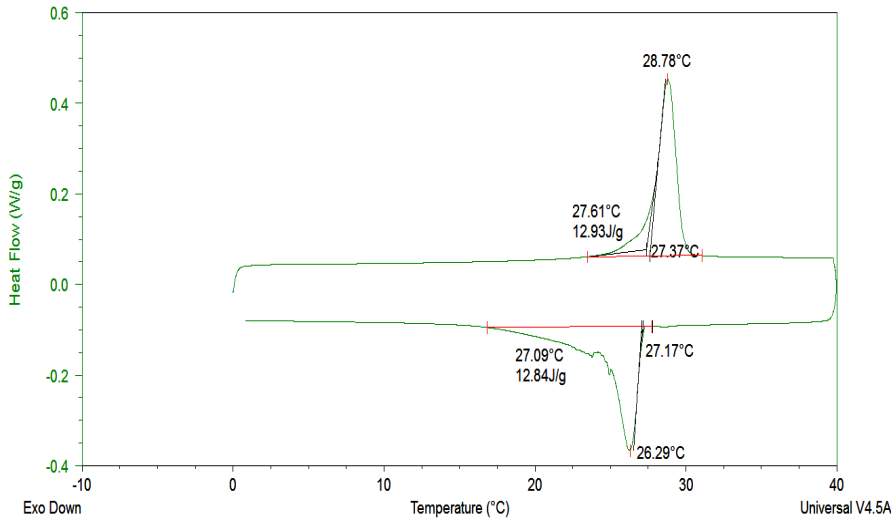

(c)

Fig. 4 DSC curves of the (a) PA, (b) PA-NC and (c) PL+PA-NC composites

B. Mechanical Performance

The flexural strength results of PL+PA-NC showed that the tested samples failed to carry the same load and broke particularly at the centre as shown in Fig. 5. The flexural strength of PL with the addition of PA-NC was considerably reduced compared to control sample of PL. The flexural strength was observed to be 1.36 MPa with reduction of 57.5% compared to control sample of PL (3.2 MPa). The reduced flexural strength of the PL+PA-NC was still acceptable according to relevant standards for building materials EN 13279-2.

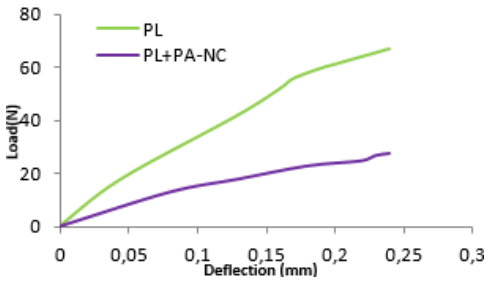

Fig. 5 Comparison of three-point bending test curves between PL samples with/without PA-NC composite

C. Flammability Testing

The curves of heat release rate (HRR) and mass loss as a function of time are graphically presented in Fig. 6. The parameters determined and derived from these curves are time to ignition (TTI), flame-out time (FOT), total mass loss, peak heat release rate (PHRR), total heat release rate (THR), and effective heat of combustion (EHC) as shown in Table I. It can be observed from the results that the PL did not burn and its THR and EHC produced were 0.5 MJ/m^2 and 0.2 MJ/kg, respectively. Whilst, PL+PA-NC ignited at 48 s after exposure to the cone heat source and burned with two peaks of heat release rate as shown in Fig. 6 (a).

The first peak of 159 kW/m^2 at 123 s is attributed to the release of PA added to PL. The second peak of 169 kW/m^2 at 370 s represents the delayed release of the PA. The THR of 51 MJ/m^2 and EHC of 8.4 MJ/kg produced from this burning are much higher than that observed in PL [9]. It can be also seen from Fig. 6 (b) that the maximum mass loss rate is 26.3% for PL+PA-NC, which is higher than that of control PL (16.5%). These results indicate that PL+PA-NC is much flammable compared to PL which did not ignite.

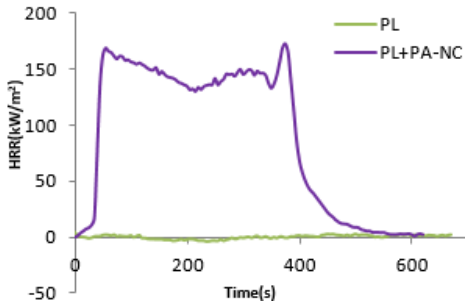

(a)

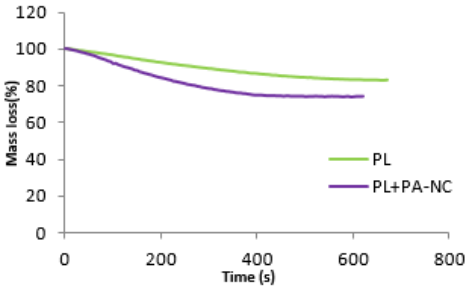

(b)

Fig. 6 Cone calorimetric results of control (PL) and PL+PA-NC at 70 kW/m^2: (a) HRR and (b) mass loss curves as a function of time

The temperature changes of the unexposed surface of sample to cone heater as a function of time during the test for 20 min were also studied, the results are shown in Fig. 7. Trends in rise of temperature in various types of samples are reflection of heat release rate versus time curves. PL had a lower temperature rise than PL+PA-NC and also it took 759 s to reach the temperature of 250 °C due to the loss of water content as a result of high temperatures generated from the cone. Hence, the coherence between PL particles was lost and the temperature started rising to reach the maximum temperature of 358 °C at 1190 s.

In case of PL+PA-NC, the temperature increased rapidly from 32 °C until the maximum temperature of 380 °C at 1106 s, which was higher than that of PL due to the ignition and burning on the surface as a result of PA and organic NC added. Furthermore, it took shorter time of 513 s to reach the temperature of 250 °C, which was attributed to the increase in heat transfer rate between both surfaces.

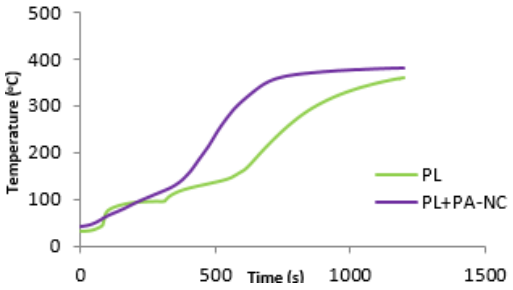

Fig. 7 Temperature versus time curves of the reverse surfaces of PL and PL+PA-NC on cone exposure at 70 kW/m^2 heat flux in vertical orientation

TABLE I
CONE CALORIMETRIC RESULTS OF CONTROL SAMPLE (PL) AND (PL+PA-NC) AT 70 KW/M EXTERNAL HEAT FLUX

Sample	TTI (s)	FO (s)	Mass loss (%)	Peak 1		Peak 2		THRR (MJ/m^2)	EHC (MJ/kg)
				PHRR (kW/m^2)	T_{PHRR} (s)	PHRR (kW/m^2)	T_{PHRR} (s)		
PL	----	-----	16.5±0.23	-----	-----	-----	-----	0.5±0.5	0.2±0.1
PL+PA- NC	48±4	467±3	26.3±0.7	159±13	123±80	169±5	370±3	51±7	8.4±0.6

D.Thermal Energy Performance

The improvement of thermal properties of the PL modified was also verified by comparing its melting and freezing performances before and after PA addition. Melting and freezing temperatures curves of the PL+PA-NC recorded at the bottom of top board are compared to those of control sample of PL as shown in Fig. 8. The melting time was taken as a time elapsed from melting point of the PA 27.5 °C to 40 °C. By similar way, the freezing time was determined as a time elapsed from the freezing point of the PA 26.6 °C to 9 °C. As can be observed from Fig. 8, the melting process took 11 min for PL, whereas it took 8 min for the PL+PA-NC. The freezing process took 38 min for PL and 35 min for PL+PA-NC. As a comparison between them, there is reduction in the melting and freezing time of the PL+PA-NC after PA addition. This is attributed to the increase in the heat transfer rate in the PL+PA-NC as a result of PA addition.

Fig. 9 represents the indoor thermal temperature variation curves of the test rooms with/without PA-NC. Due to a significant amount of heat absorbed by PA-NC enhanced PL, the temperature rate in melting process and peak temperature were lower than in the control sample. PL+PA-NC has ability to maintain a more stable indoor thermal temperature than the control sample which drops in temperature at a faster rate. In cooling process, the temperatures were reduced from 30 °C at 114 min to 9.75 °C and 7.36 °C at 166 min in the small test rooms of PL+PA-NC and PL, respectively.

The indoor thermal temperature in the small test room of PL+PA-NC was higher than that of PL by more than 2 °C due to the released heat from the PA-NC enhanced PL during cooling period. This PA-NC had an ability to store and release heat in order to reduce the energy consumption by decreasing the indoor temperature variation.

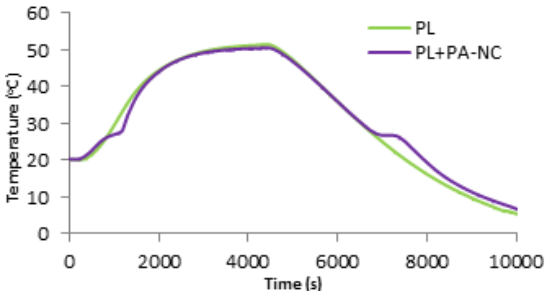

Fig. 8 Temperature versus time curves of PL with and without PA-NC during controlled heating and cooling in a chamber

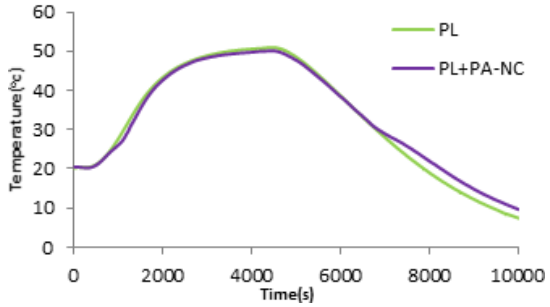

Fig. 9 Comparison of indoor temperatures curves of the small test rooms with and without PA-NC during controlled heating and cooling in a chamber

IV. CONCLUSION

The form-stable composite PA-NC was successfully prepared; the leakage test showed that the optimum mass

fraction of PA retained in the composite without leakage was 60%. The results of DSC analysis showed that the melting and freezing temperatures of PL+PA-NC and PL-NC were similar to those observed in PA, and the latent heat of PA in the PL+PA-NC decreased according to the percentage of PA added. These results indicated that the PA-NC had good latent heat to be applied for thermal energy storage in buildings. The PL prepared using PA-NC had acceptable mechanical strength. The PA-NC could reduce the indoor temperature fluctuation and had the function of maintaining warmth to reduce the building energy consumption. It can be concluded that the incorporation of PA-NC into PL increased its flammability, and the PL+PA-NC can combust easily. However, addition of these form-composites increases the flammability of the PL. To improve the flammability properties of modified PL, other flame retardant carrier materials and/or flame retardants will be explored in future work.

ACKNOWLEDGMENT

This work is financed by the General Directorate of Jordanian Civil Defence. Authors would like to express their great appreciation for this support.

REFERENCES

[1] Sharma, A., Tyagi, V. V., Chen, C. R. and Buddhi, D. "Review on thermal energy storage with phase change materials and applications", *Renewable and Sustainable Energy Reviews, 2009,* vol. 13, no. 2, pp. 318-345.

[2] Zhiqiang (John) Zhai, Miles L. L. Abarr, Saleh N. J. A. L.-Saadi and Porter Yate. "Energy Storage For Residential Buildings: Review And Advances", *APEC Conference on Low-carbon Towns and Physical Energy Storage,2013,* Changsha, China.

[3] Sari, A., Karaipekli, A. and Kaygusuz, K. "Capric acid and stearic acid mixture impregnated with gypsum wallboard for low-temperature latent heat thermal energy storage", *International Journal of Energy Research, 2008,* vol. 32, no. 2, pp. 154-160.

[4] Oliver, A. "Thermal characterization of gypsum boards with PCM included: Thermal energy storage in buildings through latent heat", *Energy & Buildings, 2011,* vol. 48, pp. 1-7.

[5] Farid, M. M., Khudhair, A. M., Razack, S. A. K. and Al-Hallaj, S. *A.* "*review on phase change energy storage: materials and applications*", Elsevier Ltd. 2004.

[6] Fang, X., Zhang, Z. and Chen, Z. "Study on preparation of montmorillonite-based composite phase change materials and their applications in thermal storage building materials", *Energy Conversion and Management, 2008,* vol. 49, no. 4, pp. 718-723.

[7] Shilei, L., Neng, Z. and Guohui, F. "Eutectic mixtures of capric acid and lauric acid applied in building wallboards for heat energy storage", *Energy & Buildings,2006,* vol. 38, no. 6, pp. 708-711.

[8] Zhang, Y., Zhang, Q., Zhou, G., Lin, K. and Di, H. "Application of latent heat thermal energy storage in buildings: State-of-the-art and outlook", *Building and Environment, 2007,* vol. 42, no. 6, pp. 2197-2209.

[9] Kandola, B. K., Alkhazaleh, A. H. and Graham J. Milnes. "The Fire Behaviour of Gypsum Boards Incorporating Phase Change Materials for Energy Storage In Building Applications", Fire and Materials Conference, San Francisco, USA, 2017.

[10] Hall, D., Donaldson, K., McAllister, J., Ross, J. A. S., Baker, D., Purser, D. A., Maynard, R. L., Wakefield, J. C., Anderson, D. and Marrs, T. "*Toxicology, Survival and Health Hazards of Combustion Products*", 1st edn, Royal Society of Chemistry, Cambridge, 2016.

[11] Alkhazaleh, A. H., and Duwairi, H. M. "Analysis of Mechanical System Ventilation Performance in an Atrium by Consolidated Model of Fire and Smoke Transport Simulation", International Journal of Heat and Technology, vol. 33 (2015), no. 3, pp. 121-126.

[12] Alkhazaleh, A. H., and Duwairi, H. M. "Modelling and Design of Smoke Control System for Regular Large Atrium Installed in Mercantile Buildings in Jordan", master thesis, university of Jordan, 2014.

[13] Guan-Yuan Wu. and Ruu-Chang Chen. "The Analysis of the Natural Smoke Filling Times in an Atrium", *Journal of Combustion, 2010,* vol. 2010, pp. 1-9.

[14] Harrison R. and Spearpoint, M J. "Smoke Management Issues in Buildings with Large Enclosures". Fire Australia, 2006, Melbourne, 1-3 November.